文章编号:2095－0411(2015)03-0001-06

Photoelectrochemical Properties of TiO_2 Nanorods Calcined from Titanate Nanorods

QU Jie, CHEN Zhihui, ZHU Yuanyuan, ZHANG Shuai, DING Jianning, YUAN Ningyi
(School of Materials Science and Engineering, Jiangsu Collaborative Innovation Center of Photovolatic Science and Engineering, Changzhou University, Changzhou 213164, China)

Abstract: Hydrothermally synthesized titanate nanorods are calcined at three different temperatures (300, 500, 700℃). The prepared samples are characterized by scanning electron microscope / transmission electron microscopy and X-ray diffraction. These samples are used to fabricate photoelectrodes for dye-sensitized solar cells. It is found from current voltage curve measurements that dye-sensitized solar cells with anatase nanorods calcined at 700℃ shows the best photoelectrochemical performance, with a photovoltaic conversion efficiency of 1.13%. Electrochemical impendence spectroscopy (EIS), intensity-modulated photocurrent spectroscopy (IMPS), and intensity-modulated voltage spectroscopy (IMVS) are used to further investigate the kinetics process of TiO_2 film electrodes. The results indicate that the anatase nanorods, calcined at 700℃, have a lower charge-transfer resistance, a faster transport time and a longer electron lifetime, implying lower electron-hole recombination and a higher charge-collection efficiency.

Key words: dye-sensitized solar cells; TiO_2; nanorod; photoelectrochemical properties

质子钛酸盐热解 TiO_2 纳米棒的光电性能研究

曲 婕, 陈智慧, 朱媛媛, 张 帅, 丁建宁, 袁宁一
(常州大学 材料科学与工程学院, 江苏省光伏科学与工程协同创新中心, 江苏 常州 213164)

摘要:为了进一步提高染料敏化太阳能电池的光电转换效率,采用水热法制备质子钛酸盐纳米棒,并在 300,500℃和 700℃下分别对上述样品烧结得到二氧化钛纳米棒。利用扫描电子显微镜和 X 射线衍射分析手段对样品进行了表征。将上述样品组装成染料敏化太阳能电池,并对其进行光电性能测试。测试结果表明 700℃烧结得到的二氧化钛纳米棒具有最高的光电转换效率为 1.13%。交流阻抗,强度调制光电流谱和光电压谱测试结果进一步显示 700℃烧结得到的锐钛矿纳米棒具有较低的电荷转移电阻,快速的电子转移速率和较长的电子寿命。上述结果表明高温烧结得到的二氧化钛纳米棒电子-空穴复合几率少,电子收集效率高,相应的光电转换效率也高。

关键词:染料敏化太阳能电池;TiO_2;纳米棒;光电性能
中图分类号:O 484 **文献标志码**:A **doi**:10.3969/j.issn.2095－0411.2015.03.001

收稿日期:2014-12-19。
基金项目:国家自然科学基金资助项目(21301022)。
作者简介:曲婕(1981—),女,山东龙口人,博士,讲师,主要从事新能源材料与器件相关领域的研究。通讯联系人:丁建宁(1966—),E-mail:dingjn@cczu.edu.cn

Dye-sensitized solar cells (DSSCs)as a promising low-cost alternative for solar energy conversion have received considerable attention as a potential cost-effective alternative [1-6]. It consists of a dye-sensitized semiconductor electrode, redox electrolyte, and counter electrode. The semiconductor electrode is the hard core among the three parts. For photovoltaic properties of dye sensitized solar cells (DSSCs), it is mainly determined by two factors, light harvesting efficiency and electron transport efficiency. Electron-transfer kinetics, which mainly competes among electron injection, recombination, and regeneration, plays an important role in the efficiency of DSSCs. Certainly the electron-transfer kinetics depends strongly on the morphology and crystal structure of semiconductor materials [7-10].

One-dimensional TiO_2 nanostructures (nanorods, and nanowires) have a relatively small amount of grain boundaries and can act as single crystal, which is able to reduce the grain boundary effect and provide fast electron transport [11-12]. However, a better understanding of the potential effect of the semiconductors structure on electron-transfer kinetics is still necessary for further improving DSSCs performance.

In this work, we calcined protonated titanate nanorods at different temperatures to make the structure transformation to TiO_2(B) nanorods and anatase nanorods. The photoelectrochemical properties of the calcined TiO_2 rods were investigated. It is found that the DSSCs with anatase nanorods calcined at 700℃ shows the highest photovoltaic conversion efficiency. This can be attributed to a lower charge-transfer resistance and a longer lifetime for the sample calcined at 700℃, as proved by EIS, IMPS and IMVS.

1 Experimental details

1.1 Sample Preparation and Characterization

The samples were prepared via the hydrothermal reaction of titanium with NaOH solution according to our previous works [13]. Anatase TiO_2 was mixed with 10mol · L^{-1} NaOH solution. After being sonicated in an ultrasonic bath for 0.5 h, the resulting suspension was transferred to a Teflon-lined autoclave and heated to 180℃ for 48h. The solid product was recovered and rinsed with distilled water, 0.1mol · L^{-1} HCl, and distilled water until pH = 7. After being dried at 60℃ for 2 days, the as-prepared sample was calcined at 300, 500, 700℃ for 2 h in air. The structure and morphology of the resultant samples were detected using X-ray diffraction (Rigaku D/max-2500) and transmission electron microscopy (FEI Tecnai 20). N_2 adsorption data were measured using a NOVA 2 000e (Quantachrome) instrument, and the specific surface area was evaluated by the Brunauer-Emmett-Teller (BET) method.

1.2 Photoelectrochemical Performance

The titanate nanorods were mixed with ethanol and stirred to obtain a fluid mixture. Then a film was made by the doctor blade method on a fluorine-doped tin (FTO) oxide conductive glass (LOF, TEC-15, 15Ω/square). After being calcined at 300, 500, 700℃ in air for 2 h, the films were soaked in an ethanol solution of N-719 dye for about 24h. The dye-adsorbed TiO_2 electrode was assembled into a sandwich-type cell with a counter electrode (platinum-sputtered FTO glass) by clamps. A drop of electrolyte solution (0.5mol · L^{-1} LiI, 0.05mol · L^{-1} I_2, and 0.5mol · L^{-1} 4-tertbutylpyridine in acetonitrile) was introduced into the clamped electrodes. The active area of the electrode was about 0.25cm^2. Photocurrent-voltage curves were measured with a Zahner IM6ex electrochemical workstation using a Trusttech CHF-XM-500W source under simulated sun illumination (Global AM 1.5, 100mW · cm^{-2}). Electrochemical impedance spectra were conducted using a Zahner IM6ex electrochemical workstation. A perturbation of 10mV was applied, and data were collected from 100 kHz to 0.1Hz. IMVS under open-circuit conditions and IMPS under short-circuit conditions were carried out using the Zahner CIMPS-2 system. The lamp house was pro-

vided with a blue-light-emitting diode (470nm) driven by a PP210 (Zahner) frequency response analyzer. The AC component of the current to the LED generated a modulation (10%) superimposed on the DC light intensity with the frequency range from 1 000 to 0.01Hz for IMPS and IMVS.

2 Results and discussion

2.1 Analysis of SEM images

As shown in Figure 1a, the sample calcined at 300℃ keeps the nanorod morphology with a length of several micrometers and diameter of about 100nm. The interference fringe spacing of the nanorods, which was measured from the high-resolution transmission electron microscopy (HRTEM) image of the sample (the insert in Figure 1a), is about 0.37nm, corresponding to the interplanar distance of the (110) plane in TiO_2 (B) phase. Nanorods of titanate are shortened when calcined at 500℃ (Figure hortened 1b). After calcination at 700℃, the nanorods become shorter and thicker.

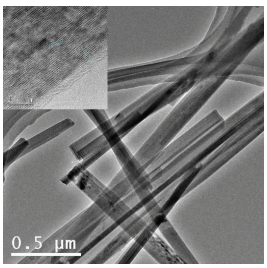

(a) 300℃

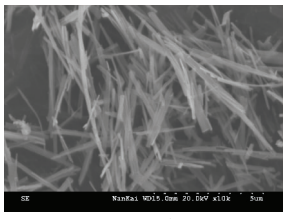

(b) 500 ℃

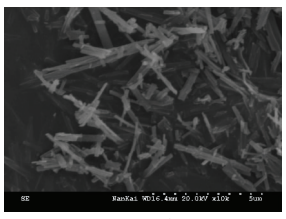

(c) 700 ℃

Fig.1 TEM image of TiO_2 nanorods obtained after calcination of titanate nanorods at different temperatures

2.2 Analysis of XRD measurements

The transformation of the crystal structure of the samples is detected by X-ray diffraction (XRD) (Figure 2). All the diffraction peaks of the sample calcined at 300℃ and 500℃ can be indexed to TiO_2 (B) (JCPDS74-1940). With calcination temperature increasing to 700℃, only the anatase phase is found in XRD patterns. Meanwhile, the peak intensities increase obviously with increasing temperature, indicating the improvement of crystallization of nanorods.

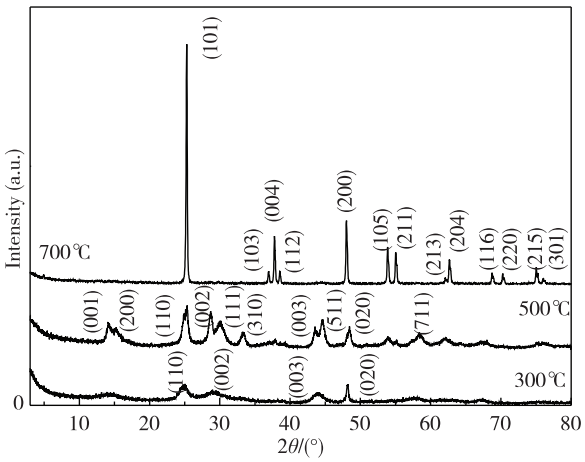

Fig.2 XRD patterns of TiO_2 nanorods obtained after calcination of titanate nanorods at different temperature

2.3 Analysis of UV-vis spectra

UV visible spectrophotometer (UV vis) absorption spectra of the samples are shown in Figure 3a. TiO_2 nanorods absorbs UV light under 380nm wavelength and has no photoresponse in the visible light region. The UV absorbance of TiO_2 (B) is obviously higher than that of anatase nanorods. The enhanced light absorption of TiO_2 (B) is attributed to the fact that it has more surface defects (relatively poor crystallization as shown in XRD patterns) than anatase phase. Figure 3b shows the UV vis absorption spectra of N-719 dye adsorbed on the nanorods calcined at different temperatures. Two main absorption peaks appear in the absorption spectra. The peak in the UV light region results from TiO_2, and the other peak at about 545 nm is ascribed to the absorption of dye N-719. Dye-absorbed TiO_2 (B) calcined at 300℃ show the highest absorption intensity in the visible light region. With the calcinations temperature rising, the absorption intensity reduces gradually. The results suggest TiO_2 (B) can adsorb a

relatively large amount of N-719 dye, due to more surface defects and higher specific surface area (the surface area for nanorods calcined at 300℃, 500, 700℃ is 19, 14 and 10$m^2 \cdot g^{-1}$ respectively).

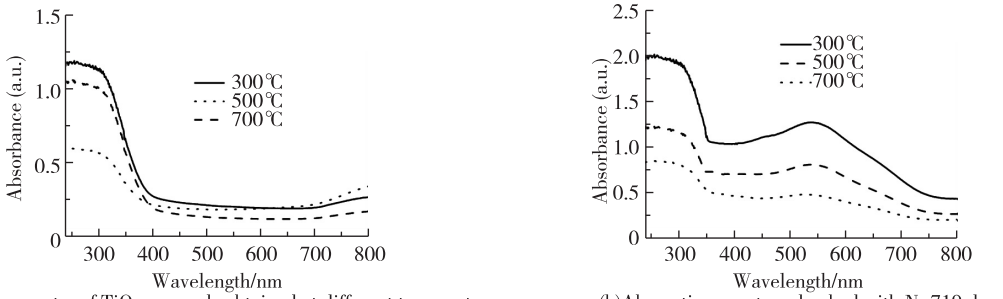

(a) Absorptionspectra of TiO_2 nanorods obtained at different temperatures (b)Absorption spectra adsorbed with N-719 dye

Fig.3 Absorptionspectra of different nanomaterials

2.4 Analysis of photoelectrochemical properties

Figure4 shows the photocurrent voltage characteristics (I-V) of the DSSCs with the nanorods calcined at 300, 500, 700℃. It can be clearly found that both short-circuit current (J_{sc}) and open-circuit voltage (V_{oc}) of the corresponding DSSCs are improved with the increase of the calcination temperature. J_{sc} and V_{oc} of the DSSCs with anatase nanorods (700℃) are up to 3.28mA · cm^{-2} and 0.78V, respectively, demonstrating the best performance. More detailed parameters are summarized in Table 1. Anatase nanorods obtained at 700℃ show the highest photovoltaic conversion efficiency, 1.13%. The photoelectrochemical performances will be further discussed in combination with the EIS results in the following discussions.

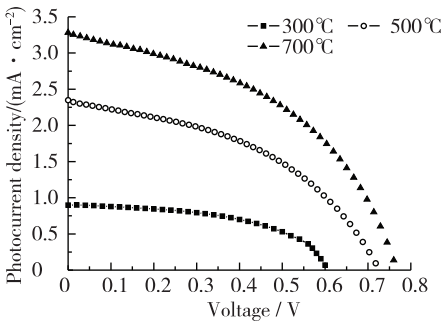

Fig.4 I-V curves for cells using different nanorods electrodes. Illumination intensity of 100mW · cm^{-2} with Global AM 1.5 and the active area of 0.25cm^2 were applied

EIS analysis could help to understand the electron kinetics of the DSSCs by analyzing the variations in impedances associated with the different configurations of applied cells [14-15]. Fig. 5 shows the typical Nyquist plot of the DSSCs. The Nyquist plots exhibited only one semicircle which corresponded to the electron transport and transfer at TiO_2/dye/electrode interface [16]. Equivalent circuit containing a constant phase element (CPE) and resistances (R_s) is used to fit the corresponding resistances (Fig. 5, inset). And the results for 300℃, 500℃ and 700℃ are 415.2, 173.6 and 74.3Ω. The charge-transfer resistance at the TiO_2/dye/electrolyte interface for nanorods calcined at different temperatures is clearly different, showing a temperature-dependent order: 300℃ > 500℃ > 700℃. Thus, the reaction activity for DSSCs also follows the temperature-dependent order: 700℃ > 500℃ > 300℃. This is in agreement with the order of the photoelectrochemical performance as presented in the photocurrent-voltage characteristic measurement.

Table 1 Detailed photovoltaic parameters of DSSCs made by TiO_2 nanorods calcined at different temperatures.

Nanorods	J_{sc}/ (mA · cm^{-2})	V_{oc}/ V	F_F	η / %	S_{BET} / ($m^2 \cdot g^{-1}$)
300℃	0.90	0.605	0.52	0.28	19
500℃	2.35	0.700	0.45	0.75	14
700℃	3.28	0.780	0.44	1.13	10

IMPS and IMVS were used further to investigate the electron transport and recombination processes, as shown in Figure 6. The electron collection time (τ_d) and the recombination time (τ_n) can be estimated from the IMPS plots and the IMVS plots, respectively [17]. The detailed param-

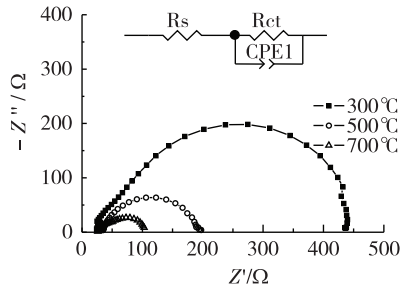

Fig. 5 Impedance spectra of DSSCs made of TiO_2 nanorods calcined at different temperatures. The inset shows the equivalent circuit for the impedance spectrum. Rct: charge-transfer resistance of TiO_2/dye/electrolyte interface; CPE: constant phase element.

eters are listed in Table 2. It is found that τ_n increased with the calcination temperatures rising, showing a clear order: 700℃ > 500℃ > 300℃ and τ_d shows the reverse order: 300℃ > 500℃ > 700℃. A short electron transport time means fast electron transport process in the photoanode film, and low probability of electron recombination, and a long lifetime means enough time for electrons to transport, which are important to improve charge-collection efficiency and energy conversion efficiency of DSSCs [18]. The above results indicate nanorods calcined at 700℃ show the optimized fast reaction kinetics. It is considered that the good crystallinity and the cylindrical geometry could allow the nanorods to support radial electric fields that could keep the electrons away from the nanorods surface, thereby reducing surface electron densities and recombination[11]. Anatase nanorod show better crystallinity and less defects than TiO_2(B) nanorod, for which more electron could be survived.

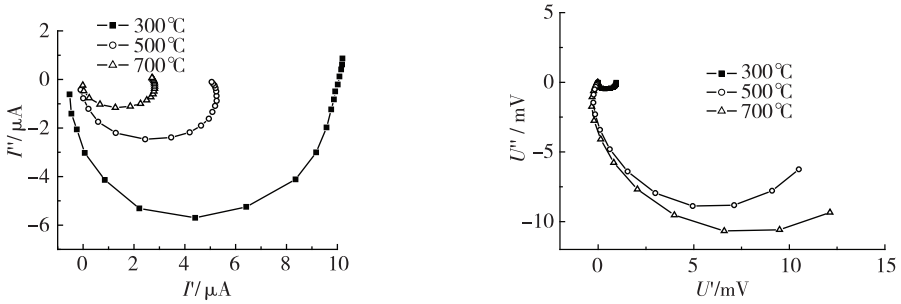

(a) Short-circuit IMPS response (b) IMVS response

Fig.6 Short-circuit Imps and IMVS response with different materials

Table 2 Detailed IMPS/IMVS parameters of DSSCs made by TiO_2 nanorods calcined at different temperatures.

NR	τ_d/ ms	τ_n/ ms
300℃	2.07	19.70
500℃	1.46	54
700℃	0.94	93.7

3 Conclusion

After calcination at different temperatures, the synthesized titanate nanorods can be converted to TiO_2(B) nanorods and anatase nanorods. Anatase nanorods calcined at 700℃ show better photoelectrochemical performance than TiO_2(B) nanorods, and the corresponding DSSCs has the photovoltaic conversion efficiency of 1.13%. EIS, IMPS and IMVS indicate that the anatase nanorods calcined at 700℃ have a lower charge-transfer resistance, faster electron transport and longer electron lifetime, due to its unique morphology and structure. The results are very significant for further understanding the effects of the morphology and crystalline structure of photoelectrode materials on photoelectrochemical properties, and for the design of efficient photoanode materials with optimum structures for DSSCs.

References:

[1]GRÄTZEL M. Conversion of sunlight to electric power by nanocrystalline dye-sensitized solar cells[J]. Journal of Photochemistry and Photobiology A: Chemistry, 2004, 164: 3-14.

[2] QU J, YANG Y, WU Q, et al. Hedgehog-like hierarchical ZnO needle-clusters with superior electron transfer kinetics for dye sensitized solar cells[J]. RSC Advances, 2014(4):11430-11437.

[3] PAGLIARO M, PALMISANO G, CIRIMINNA R, et al.

Nanochemistry aspects of titania in dye-sensitized solar cells[J]. Energy & Environmental Science, 2009(2): 838-844.

[4]奚小网,胡林华,方霞琴,等.TiO_2薄膜优化对染料敏化太阳电池性能的影响[J].无机化学学报, 2011,27(7) :1353-1357.

[5] 梅翠玉,王小平,王丽军,等.染料敏化太阳能电池的研究进展[J].材料导报,2011,25(13) :148-152.

[6]程存喜,林建明,肖尧明,等. TiO_2纳米线的制备及在柔性染料敏化太阳能电池中的应用[J]. 厦门大学学报(自然科学版),2011, 50(Z1):105-108.

[7] GRÄTZEL M. Photoelectrochemical cells[J]. Nature, 2001, 414: 338-344.

[8] HAQUE S A, PALOMARES E, CHO B M, et al. Charge separation versus recombination in dye-sensitized nanocrystalline solar cells: the minimization of kinetic redundancy[J]. Journal of the Americian Chemical Society, 2005, 127: 3456-3462.

[9] QIAN J F, LIU P, XIAO Y, et al. Beyond one-electron reaction in li cathode materials: designing Li_2 MnxFe$_{1-x}$ SiO_4 [J]. Advanced Materials, 2009, 21: 3633-3640.

[10] BIERMAN M J, JIN S. Potential applications of hierarchical branching nanowires in solar energy conversion[J]. Energy & Environmental Science, 2009, 2: 1050-1059.

[11] MIAO C, CHEN C, DAI Q, et al. Dysprosium, holmium and erbium ions doped indium oxide nanotubes as photoanodes for dye sensitized solar cells and improved device performance[J]. Journal of Colloid And Interface Science, 2015, 440: 162-167.

[12] KANG S H, CHOI S H, KANG M S, et al. Nanorod-based dye-sensitized solar cells with improved charge collection efficiency[J]. Advanced Materials, 2008, 20: 54-58.

[13] QU J, GAO X P, LI G R, et al. Structure Transformation and photoelectrochemical properties of tio_2 nanomaterials calcined from titanate nanotubes[J]. Journal of Physics Chemistry C, 2009, 113: 3359-3363.

[14] SHAN C H, SANG X J, ZHANG H, et al. Enhanced DSSC performance with tri-pyridine-ruthenium heteropolytungstate[J]. Inorganic Chemistry Communications, 2014, 50: 13-16.

[15] ITAGAKI M, HOSHINO K, NAKANO Y, et al. Faradaic impedance of dye-sensitized solar cells[J]. Journal of Power Sources, 2010, 195: 6905-6923.

[16] HAN L Y, KOIDE N, CHIBA Y, et al. Modeling of an equivalent circuit for dye-sensitized solar cells[J]. Applied Physics Letter, 2004, 84: 2433-2435.

[17] FRANCO G, GEHRING J, PETER L M, et al. Frequency-resolved optical detection of photoinjected electrons in dye-sensitized nanocrystalline photovoltaic cells[J]. Journal of Physics Chemistry B, 1999, 103: 692-698.

[18] PETER L M, WIJAYANTHA K G U. Variation of carboxylate-functionalized cyanine dyes to produce efficient spectral sensitization of nanocrystalline solar cells[J]. Electrochimica Acta, 2000, 45: 4543-4551.

(责任编辑:李艳)